

Multi-level Latent Space Structuring for Generative Control

OREN KATZIR, Tel Aviv University
 VICKY PEREPELOOK, Tel Aviv University
 DANI LISCHINSKI, Hebrew University of Jerusalem
 DANIEL COHEN-OR, Tel Aviv University



Fig. 1. Multi-level structuring of StyleGAN’s intermediate latent space, \mathcal{W} . Specifically, we group the layers of StyleGAN’s generator layers into three levels: coarse (C), medium (M) and fine (F), and learn a set of clusters for each level. Each of the three groups above corresponds to a different coarse-level cluster, where each row is from the same medium-level cluster, and each column is from the same fine-level cluster.

Truncation is widely used in generative models for improving the quality of the generated samples, at the expense of reducing their diversity. We propose to leverage the StyleGAN generative architecture to devise a new truncation technique, based on a decomposition of the latent space into clusters, enabling customized truncation to be performed at multiple semantic levels. We do so by learning to re-generate \mathcal{W}^L , the extended intermediate latent space of StyleGAN, using a learnable mixture of Gaussians, while simultaneously training a classifier to identify, for each latent vector, the cluster that it belongs to. The resulting truncation scheme is more faithful to the original untruncated samples and allows better trade-off between quality and diversity. We compare our method to other truncation approaches for StyleGAN, both qualitatively and quantitatively.

1 INTRODUCTION

Generative Adversarial Networks (GANs) [Goodfellow et al. 2014] have dramatically transformed unconditional image synthesis. In particular, models based on the recent StyleGAN architecture [Karras et al. 2019, 2020] have demonstrated an impressive ability to generate images of unprecedented photorealism. One distinguishing feature of such generative models is that they learn a mapping from the original latent space, which is typically normally distributed, to an intermediate latent space \mathcal{W} , which is claimed to better mimic the distribution of the training data.

Realizing that \mathcal{W} is not a simple normal distribution suggests that it is beneficial to understand and make use of the particular structure of this space. In this paper, we explore the idea of imposing structure on the intermediate latent space in a more explicit manner. More specifically, given a pretrained generator, we learn new mappings that give rise to a collection of clusters in the latent

space. Furthermore, three different collections of clusters are used to control the coarse, medium, and fine generator levels. We show that structuring the intermediate latent space in this manner offers several benefits, particularly when dealing with image datasets that exhibit high diversity or multi-modality.

One of the resulting advantages of discovering such a multi-level structure of the latent space is the ability to perform latent space truncation in a more sophisticated manner. Truncation essentially trades off the diversity of the generated samples for their realism. We demonstrate that performing truncation while taking into account the clustered structure of the latent space yields more realistic results in return for a significantly smaller sacrifice of diversity.

Another advantage lies in our learned mapping functions. These mapping functions allow better control on the generation process by selecting for each level of styleGAN generator a specific cluster, or multiple clusters, changing different attributes in the generated image, as shown in Figure 1.

We compare our method with the original styleGAN [Karras et al. 2019] truncation to demonstrate the effectiveness of our approach both qualitatively and quantitatively.

2 RELATED WORK

Multi-modal generation. features three main approaches. The common one is to construct a continuous multi-modal latent space usually in the form of a GMM, where each of the Gaussians should capture a different modality [Gurumurthy et al. 2017; Ben-Yosef and Weinshall 2018; Pandeva and Schubert 2019]. The second approach is to combine a continuous latent space (i.e. a Gaussian distribution)

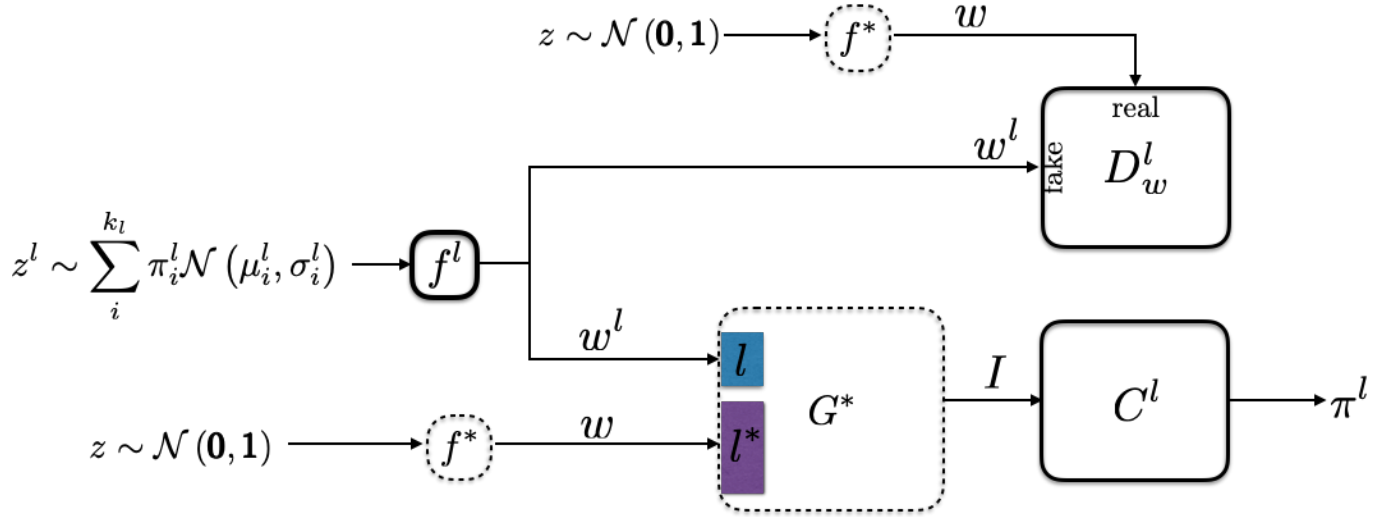


Fig. 2. Single level latent architecture. We train, independently, for each level l of styleGAN, a new mapping network f^l and level Discriminator D_w^l to generate $w^l \in \mathcal{W}$. We encourage a multi-modal distribution by feeding the original styleGAN generator G , with the new learned w^l only to level l while other level are fed with a random $w \in \mathcal{W}$. Simultaneously, The classifier C^l is trained to reconstruct each mode π^l . Please note that styleGAN original mapping function and image generator are pre-trained and fixed (drawn in dashed lines).

with a discrete, one-hot vector, where the latter indicates the different modalities [Mukherjee et al. 2019; Liu et al. 2020; Chen et al. 2016]. The third is to over-parameterize the generative model by a mixture of generators [Ghosh et al. 2018; Khayatkhoei et al. 2018; Hoang et al. 2018]. The multi modality generative learning, could be completely unsupervised, i.e. assuming the adversarial generation will tend to produce such modalities, or it is self-supervised, usually by introducing an encoder which reconstructs the selected modality index (i.e. the gaussian index, the one-hot encoding or the selected generator). Differently, in Liu *et al.* [Liu et al. 2020] the modes in the latent space are not modeled but derived from clustering the corresponding discriminator features of the generated images. Sendik *et al.* [Sendik et al. 2020] extend StyleGAN to learn k constants corresponding to different modes in the data. Since the above approaches were applied on the input to the convolution layers, they usually extract very different modes and do not offer control at different semantic levels.

Style-based generative adversarial networks. Style-based generative models [Karras et al. 2019, 2020] have paved the way for a variety of applications, most of them rooted in the added control that the learned intermediate latent space \mathcal{W} has on the generated model. In contrast to \mathcal{W} , where the same vector is injected to all of the StyleGAN generator layers, an extended \mathcal{W}^+ space was found to enable embedding of a much wider range of images [Abdal et al. 2019] into the StyleGAN latent space. With a correct set of constraints, this allows high-quality image editing, even for out-of-training-distribution images. Our learned modalities are also learned in an extended version of \mathcal{W} .

Evaluation of generative models. All evaluation methods first feed-forward both real and generated images in a pre-trained network (usually inception_v3 [Szegedy et al. 2016]), to extract semantically

meaningful features. The most commonly used evaluation metrics are FID [Heusel et al. 2017], IS [Salimans et al. 2016] and KID [Arbel et al. 2018]. However, since these metrics combine both quality and variety measures into a single number, it is hard to fully assess the quality of a generative model. Therefore, the notion of precision and recall for generative models was proposed [Sajjadi et al. 2018]. Following the same notion, a state-of-the-art method was proposed in [Kynkäänniemi et al. 2019], quantifying the precision/recall by measuring how many generated/real images are within the real/generated image manifold.

Truncation. Truncation is a post-training method, sacrificing the variety of a generative model to increase the quality of individual samples. The most well-known truncation method is the “truncation trick” [Marchesi 2017; Brock et al. 2018]: sampling from a truncated normal distribution at test time. This simple procedure had shown to dramatically boost the results in BigGAN [Brock et al. 2018]. Instead of truncating the distribution, [Kingma and Dhariwal 2018] proposed to sample the latent space from a reduced-temperature probability at test time. Similarly, generative models based on StyleGAN architectures [Karras et al. 2019, 2020] adopted a simple truncation operation in \mathcal{W} space. However, instead of truncating the learned manifold in \mathcal{W} , Karras *et al.* [Karras et al. 2019] scale the deviation of specific $w \in \mathcal{W}$ from the global mean by a fixed factor. Another approach [Kynkäänniemi et al. 2019] clamps samples in low-density areas to the boundary of high-density areas. Such clamping was shown to outperform the linear interpolation toward the mean. Assuming that the Frobenius norm of the generator’s Jacobian is high in low-density areas, [Tanielian et al. 2020] truncate by rejecting such samples. The latter is a binary rejection method, whereas we are interested in improving poor samples, rather than discarding them altogether.

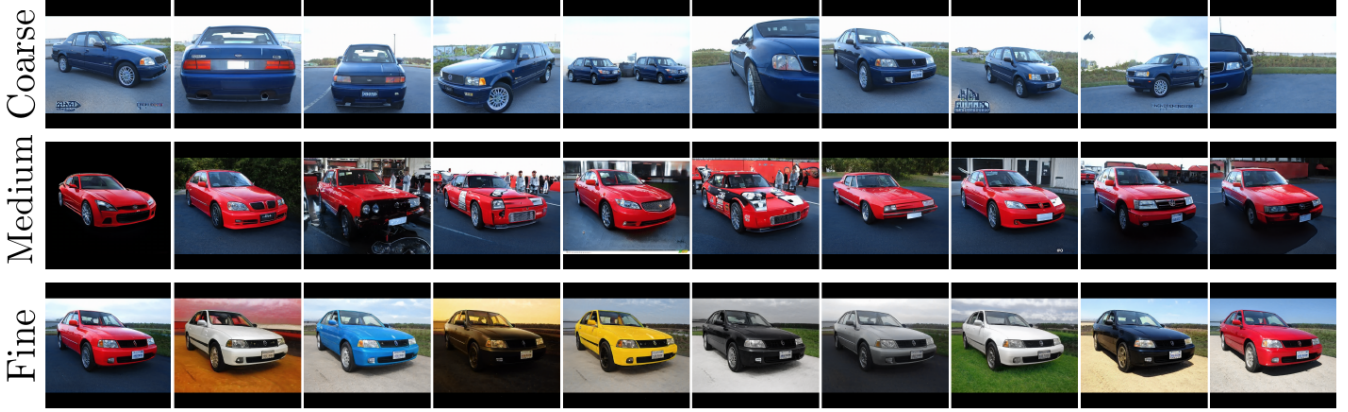


Fig. 3. The semantics controlled by different latent levels for StyleGAN trained on the LSUN-cars dataset [Kramberger and Potočník 2020]. Coarse layers control the view point and/or car pose, while medium layers control the shape of the car and the background appearance. The fine layers control mainly the colors.

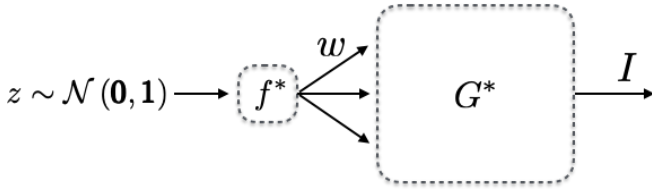


Fig. 4. A high-level view of the StyleGAN architecture. A single latent space vector $w \in \mathcal{W}$ generates the style parameters for all the levels of the generator.

3 METHOD

We propose a new truncation scheme, based on learned clusters in latent space. Given a pre-trained StyleGAN model, we cluster its learned intermediate latent space into k clusters. However, for improved control at different semantic levels, we cluster an extended latent space \mathcal{W}^L , where $L \in [1 : 18]$ (using this notation \mathcal{W}^1 is the original \mathcal{W} space and \mathcal{W}^{18} is the \mathcal{W}^+ space [Abdal et al. 2019]). Specifically, we independently cluster each semantic level $l \in [1, \dots, L]$, and preform truncation against the predicted cluster of $w \in \mathcal{W}^l$, which is, by definition, different for every semantic level. Our overall architecture is shown in Figure 2.

3.1 Semantic clustering of a pre-trained StyleGAN

In the StyleGAN architecture, as shown in Figure 4, a single $w \in \mathcal{W}$ is fed to all levels of the generator G , thus, a single latent vector w controls both high level features and low-level features in the generation process. Consequently, simple clustering methods in \mathcal{W} , such as Gaussian Mixture Models (GMM), typically cluster similar view points or similar scale of the image, but do not reflect any grouping of images based on their medium- or low-level semantic content, as demonstrated in Figure 5.

To learn a more fine-grained semantic clustering, we propose to examine each semantic level \mathcal{W}^l of the extended latent space



Fig. 5. Clustering \mathcal{W} using a Gaussian Mixture Model (GMM). The centers of the clusters reflect that the grouping is according to high-level semantics (view-point and car orientation), rather than according to medium or low-level semantics.

separately. We model each \mathcal{W}^l as a multi-modal space, and learn a new mapping network f^l to generate it as such. Following [Hoang et al. 2018], we feed f^l with learnable gaussians $\{\mu_i^l, \sigma_i^l\}_{i=1}^{k_l}$, and simultaneously learn to infer the input Gaussian π_i^l . In practice, $\pi_i^l \in \{0, 1\}$ and we use a classification network C^l to infer which Gaussian generated each $w^l \in \mathcal{W}^l$. Note that the pretrained generator G is kept fixed in this process. Since G was trained to generate images from vectors in \mathcal{W} , we use a discriminator D_w^l , to ensure that \mathcal{W}^l is similar to \mathcal{W} . We adopt WGAN-GP [Gulrajani et al. 2017] as our adversarial loss, and cross-entropy as the classification loss. The overall loss for layer l is:

$$\begin{aligned} \min_{f^l, C^l, \{\mu_i^l, \sigma_i^l\}_{i=1}^{k_l}} \max_{D_w^l} E_{w \sim \mathbb{P}_w} [D_w^l(w)] \\ - E_{w^l \sim \mathbb{P}_{f^l}, \pi^l \sim \mathbb{P}_{\pi^l}} [D_w^l(w^l) - \log(\pi^l C^l(G(w^l)))] \\ + \lambda_{gp} E_{w \sim \mathbb{P}_w, w^l \sim \mathbb{P}_{f^l}} L_{gp}(D, w, w^l), \end{aligned}$$



Fig. 6. Mean of \mathcal{W} next to several random samples for two diverse datasets. When the datasets exhibit great diversity at multiple semantic levels, a single mean can not represent the desired target to interpolate towards, due to significant differences in high-level semantics (view point, shape) as well as low-level semantics (color, texture).

where $w^l = f\left(\sum_{i=1}^{k_l} \pi_i^l \mathcal{N}(\mu_i, \sigma_i)\right)$, $\mathbb{P}_{\pi^l}(\pi^l = e_i) = 1/k_l$ for $i = 1, \dots, k_l$ and L_{gp} is the gradient penalty on straight line between w and w^l as defined in [Gulrajani et al. 2017].

3.2 Hierarchy of clusters

We train independently for each level l a new mapping function f^l with k_l clusters, to expose $\sum_l k_l$ semantic clusters. While the selection of the levels can be done arbitrarily, since we are interested in semantically meaningful clusters, we have found it beneficial to use only $L = 3$ (i.e. we generate in \mathcal{W}^3 space), where $l = 1$ is the coarse, high-level semantic layer, typically representing view point and scale, $l = 2$ is the medium-level semantics, representing background and high shape deformation (e.g. a model of a car) constrained on the coarse layer, and the fine layer, $l = 3$, representing low level semantics, such as textures and colors. In Figure 3 we demonstrate these three semantic levels for the LSUN-cars dataset. The exact mapping between the StyleGAN generator layers and the three levels of \mathcal{W}^3 is reported in the supplementary material.

3.3 Cluster-based truncation

The basic truncation scheme used by StyleGAN, assumes that contracting the latent space \mathcal{W} towards the mean improves the output image. This is based on the assumption, that denser areas in the latent space, represent higher quality images. However, while a single mean is perhaps a valid assumption for arguably unimodal datasets such as FFHQ [Karras et al. 2019], when the generated data is multi-modal the assumption does not hold. In Figure 6 we show the mean and next to it a few random samples for two diverse datasets (LSUN-cars and LSUN-horses), to demonstrate that a single mean cannot represent well the different samples in such datasets.

We propose to utilize the learned clusters in order to develop a novel, more sophisticated, multi-level semantic truncation scheme. Given $w \in \mathcal{W}$, we first determine, for each semantic level, which cluster it belongs to. Since there are k_l clusters at each level l , the total number of possible outcomes (combinations of cluster assignments) is $\prod_l k_l$ clusters, as illustrated in Figure 7.

Next, for each cluster, we perform a contraction of w towards the corresponding cluster mean, and concatenate them to yield $w_{trunc} \in \mathcal{W}^3$. The truncation procedure is summarized in Alg. 1.

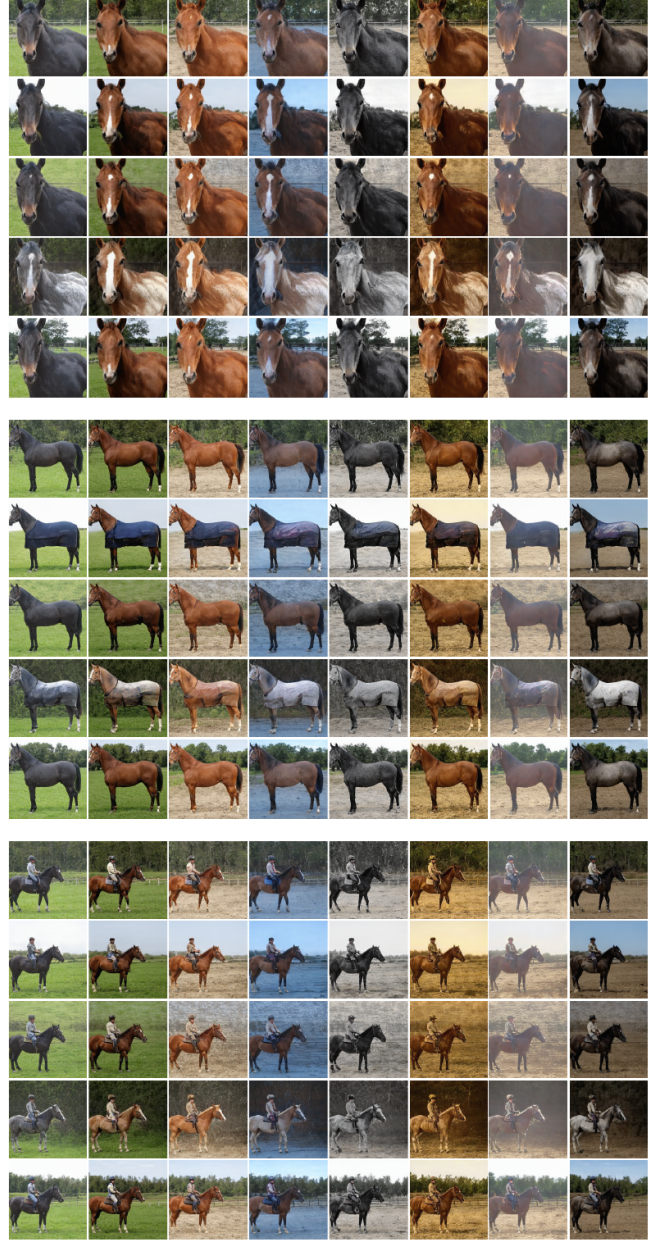


Fig. 7. Combinations of different semantic clusters. Each of the three groups of images corresponds to a different high-level cluster. In each group, the rows and columns represent five different medium-level and eight fine-level clusters, respectively.

4 EXPERIMENTS

We evaluate the proposed truncation method on LSUN [Yu et al. 2015] horses and cars. Both datasets exhibit high diversity both in global geometric features (pose, semantic content, background features), and in color and texture (object color, global brightness,



Fig. 8. Comparison of styleGAN truncation (upper row) and our semantic truncation (lower row). The images on the left, are truncated using styleGAN center (upper row) and our semantic centers (right). Our truncation generates images, closer to the original image, preserving the viewpoint and the semantic content (number of cars, part of the animal, etc.)

Algorithm 1: Multi-level semantic truncation

Result: Truncated latent vector $w_{trunc} \in \mathcal{W}^3$

Input: Latent vector $w \in \mathcal{W}$, mean of clusters for each level

$\left\{ \left\{ w_{c_i}^l \right\}_{i=1}^{k_l} \right\}_{l=1}^L$, truncation strength ϕ ;

Initialize: $w_{trunc} \leftarrow []$;

for l in $[1, \dots, L]$ **do**

$i \leftarrow \arg \max_i \{ C^l(w)[i] \}$;

$w_l \leftarrow w + \phi (w_{c_i}^l - w)$;

$w_{trunc} \leftarrow [w_l | w_{trunc}]$;

end

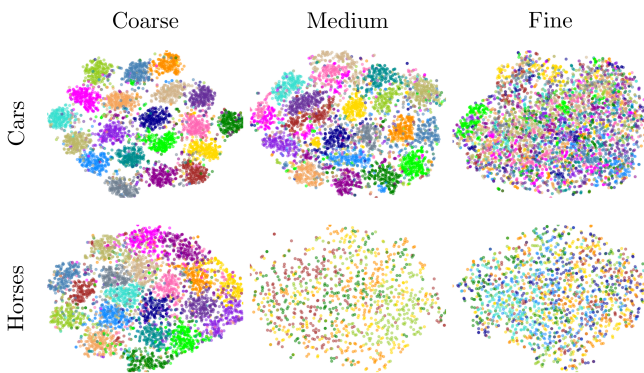


Fig. 9. TSNE of \mathcal{W} for different semantic levels. Each color represent different learned cluster by our architecture. While the coarse layer exhibit noticeable clusters, the fine layer does not, indicating that distances in \mathcal{W} has less low level semantic meaning.

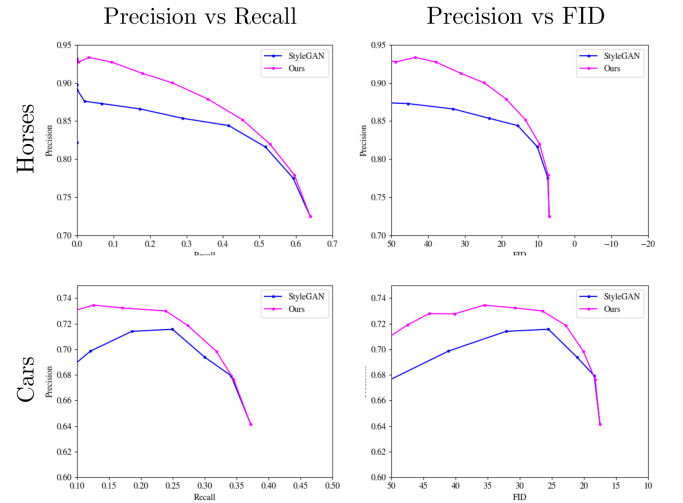


Fig. 10. PR curves.

texture patterns). In all experiments, we have used the official pre-trained StyleGAN2 generator [Karras et al. 2020]. Since these pre-trained generators, were trained to generate different sizes of images (256×256 for horses and 512×512 for cars), they have a different amount of convolution layers (14 and 16 respectively). In all our experiments, we have used 3 semantic levels w^l ($l = 1 \dots 3$). Our coarse mapping function, generating w^0 feeds the first 4 convolution layers of the StyleGAN2 generator. The medium semantic level mapping function is fed to the next 4 convolution levels. The fine mapping function is fed to the remaining layers, but the last one. We have found that assigning the last layer of StyleGAN2 generator to our fine level w^2 leads to artifacts, thus, we feed the last convolution

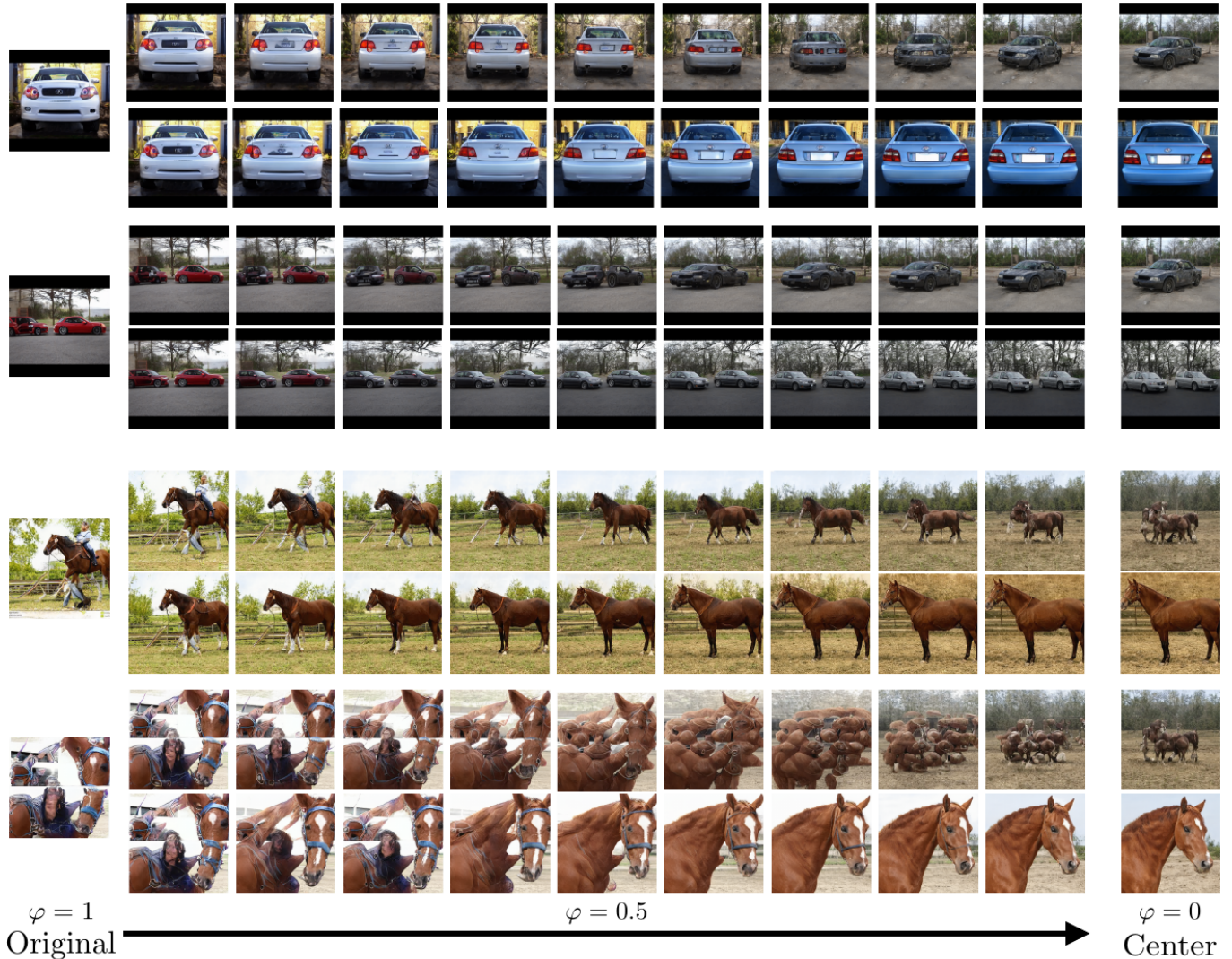


Fig. 11. Comparison of styleGAN truncation (upper row) and our semantic truncation (lower row). The images on the left, are truncated using styleGAN center (upper row) and our semantic centers (right). Our truncation generates images, closer to the original image, preserving the viewpoint and the semantic content (number of cars, part of the animal, etc.)

layer with vector $w \in \mathcal{W}$ from the original styleGAN mapping function, thereby limiting our fine mapping function to control only 7 and 5 layers for the cars and horses generators, respectively. We have trained our multi-modal mapping functions, classifier, and discriminator for 10000 iterations, with batch size 4, where all semantic levels for a specific dataset were trained independently but simultaneously.

4.1 Multi-level controlled generation

Our learned mapping functions per level, also enable us to control the generation process. Specifically, we can alternate at a specific level between different clusters. As these clusters are from the same level, the difference between them is limited to specific attributes.

In Figure 8 we show an example of such control. We first generate a specific w^0, w^1, w^2 for the coarse, medium, and fine levels respectively, from a specific cluster in each level, yielding a single image. Then, we sample a new latent code from a different cluster in a single level, while fixing other levels' latent codes. The result is a different version of the same image, corresponding to the control of the levels and the learned clusters Figure 8.

4.2 Evaluating the modalities

Our learned modalities are driven by a classifier in the image domain, while our architecture drives each level of clusters to capture modalities at different semantic level. In Figure 9 we observe the correlation between these clusters and the Euclidean distance in

\mathcal{W} . We randomly select 1000 latent vector z of every cluster and feed forward them through our learned mapping function. We then reduce the dimension by t-SNE, separately for each level. As can be seen in Figure 9, the coarse level exhibit high correlation in \mathcal{W} (i.e. clusters can be observed), while the fine level clusters are not observable in \mathcal{W} at all. The meaning of this results, is that \mathcal{W} is not a good space to measure the distance between low level semantic.

4.3 Truncation

We leverage our learned latent clusters to preform our multi-level truncation procedure, as described in Section 3.3 and Alg. 1. We calculate, for each cluster i at level l it's center i , $w_{c_i}^l$ by clustering $N = 10000$ samples of $w \in \mathcal{W}$. To evaluate the quality of our truncation methods, we preform truncation at different "strength" and evaluate the quality of the generated samples.

Quantitative comparison. To quantitatively compare our method with StyleGAN we follow the procedure proposed in [Kynkäänniemi et al. 2019]. We first randomly sample 10,000 images from the dataset. Similarly, we generate the same amount of latent vectors $w \in \mathcal{W}$, and their corresponding images, $I = G(w)$. We then cluster each w at every level (i.e. coarse, medium and fine). The "strength" of the truncation is varied by sampling 11 values in the range of $\varphi \in (0, 1)$. For each value we truncate the pre-sampled $w \in \mathcal{W}$, using both StyleGAN truncation and our semantic truncation and generate the corresponding images. These generated images are then feed-forwarded through Inception-v3 [Szegedy et al. 2016] pre-trained on ImageNet until the last fully-connected layer. For each φ we calculate the precision, recall and FID [Heusel et al. 2017] as defined in [Kynkäänniemi et al. 2019], and accumulate the results to a PR-curve and a P-FID curve as shown in Figure 10. As can be seen, our truncation achieves higher precision for the same FID and Recall compared with the standard StyleGAN truncation.

Qualitative comparison. We show the quality of our truncation method, compared to the original StyleGAN truncation in Figure 11. While StyleGAN truncation does improve the quality of the results, the contraction to a specific mean, reduces the variability, both for high-level semantics (shape, scale) and low-level semantics (background, color). Our truncation on the other hand allows a more detailed approach, where first the appropriate center is selected for each level, thus enabling more variability in each level, but moreover, most of the truncation results, while improving the quality, remain faithful to the original image in term of the pose, semantic content, background, and color as shown in Figure 11.

5 CONCLUSIONS

We proposed a new truncation technique, based on a decomposition of the latent space into clusters, at different levels of the extended latent space \mathcal{W}^L . We showed that such truncation improves previous results both qualitatively and quantitatively, producing faithful output to the original un-truncated image. Our re-arrangement of the latent space also allows a more controlled generation by selecting the desired cluster at each level. We believe that this new arrangement paves future research for methods that aim to edit images by inverting to styleGAN latent space. As editing requires an inversion

mechanism to generate a single $w \in \mathcal{W}$ for all levels, our method may remove such constraint by requiring only inversion to different clusters at different levels.

REFERENCES

- Rameen Abdal, Yipeng Qin, and Peter Wonka. 2019. Image2stylegan: How to embed images into the stylegan latent space?. In *Proceedings of the IEEE/CVF International Conference on Computer Vision*. 4432–4441.
- Michael Arbel, Dougal J Sutherland, Mikołaj Bińkowski, and Arthur Gretton. 2018. On gradient regularizers for MMD GANs. *arXiv preprint arXiv:1805.11565* (2018).
- Matan Ben-Yosef and Daphna Weinshall. 2018. Gaussian Mixture Generative Adversarial Networks for Diverse Datasets, and the Unsupervised Clustering of Images. *arXiv preprint arXiv:1808.10356* (2018). arXiv:1808.10356 [cs.LG]
- Andrew Brock, Jeff Donahue, and Karen Simonyan. 2018. Large scale GAN training for high fidelity natural image synthesis. *arXiv preprint arXiv:1809.11096* (2018).
- Xi Chen, Yan Duan, Rein Houthoof, John Schulman, Ilya Sutskever, and Pieter Abbeel. 2016. InfoGAN: Interpretable representation learning by information maximizing generative adversarial nets. *arXiv preprint arXiv:1606.03657* (2016).
- Arnab Ghosh, Viveka Kulharia, Vinay P Nambodiri, Philip HS Torr, and Puneet K Dokania. 2018. Multi-agent diverse generative adversarial networks. In *Proc. CVPR*. 8513–8521.
- Ian J. Goodfellow, Jean Pouget-Abadie, Mehdi Mirza, Bing Xu, David Warde-Farley, Sherjil Ozair, Aaron Courville, and Yoshua Bengio. 2014. Generative Adversarial Nets. In *Proceedings of the 27th International Conference on Neural Information Processing Systems - Volume 2* (Montreal, Canada) (NIPS'14). MIT Press, Cambridge, MA, USA, 2672–2680.
- Ishaan Gulrajani, Faruk Ahmed, Martin Arjovsky, Vincent Dumoulin, and Aaron Courville. 2017. Improved training of wasserstein gans. *arXiv preprint arXiv:1704.00028* (2017).
- Swaminathan Gurumurthy, Ravi Kiran Sarvadevabhatla, and R. Venkatesh Babu. 2017. DeLiGAN: Generative adversarial networks for diverse and limited data. In *Proc. CVPR*. 166–174.
- Martin Heusel, Hubert Ramsauer, Thomas Unterthiner, Bernhard Nessler, Günter Klambauer, and Sepp Hochreiter. 2017. GANs Trained by a Two Time-Scale Update Rule Converge to a Nash Equilibrium. (2017).
- Quan Hoang, Tu Dinh Nguyen, Trung Le, and Dinh Phung. 2018. MGAN: Training generative adversarial nets with multiple generators. In *Proc. ICLR*.
- Tero Karras, Samuli Laine, and Timo Aila. 2019. A style-based generator architecture for generative adversarial networks. In *Proc. CVPR*. 4401–4410.
- Tero Karras, Samuli Laine, Miika Aittala, Janne Hellsten, Jaakko Lehtinen, and Timo Aila. 2020. Analyzing and improving the image quality of stylegan. In *Proc. CVPR*. 8110–8119.
- Mahyar Khayatkhoei, Ahmed Elgammal, and Maneesh Singh. 2018. Disconnected manifold learning for generative adversarial networks. *arXiv preprint arXiv:1806.00880* (2018).
- Diederik P Kingma and Prafulla Dhariwal. 2018. Glow: Generative flow with invertible 1x1 convolutions. *arXiv preprint arXiv:1807.03039* (2018).
- Tin Kramberger and Božidar Potočnik. 2020. LSUN-Stanford Car Dataset: Enhancing Large-Scale Car Image Datasets Using Deep Learning for Usage in GAN Training. *Applied Sciences* 10, 14 (2020), 4913.
- Tuomas Kynkäänniemi, Tero Karras, Samuli Laine, Jaakko Lehtinen, and Timo Aila. 2019. Improved precision and recall metric for assessing generative models. *arXiv preprint arXiv:1904.06991* (2019).
- Steven Liu, Tongzhou Wang, David Bau, Jun-Yan Zhu, and Antonio Torralba. 2020. Diverse image generation via self-conditioned GANs. In *Proc. CVPR*. 14286–14295.
- Marco Marchesi. 2017. Megapixel size image creation using generative adversarial networks. *arXiv preprint arXiv:1706.00082* (2017).
- Sudipto Mukherjee, Himanshu Asnani, Eugene Lin, and Sreeram Kannan. 2019. ClusterGAN: Latent space clustering in generative adversarial networks. *Proceedings of the AAAI conference on artificial intelligence* 33, 01 (2019), 4610–4617.
- Teodora Pandevara and Matthias Schubert. 2019. Mmgan: Generative adversarial networks for multi-modal distributions. *arXiv preprint arXiv:1911.06663* (2019).
- Mehdi SM Sajjadi, Olivier Bachem, Mario Lucic, Olivier Bousquet, and Sylvain Gelly. 2018. Assessing generative models via precision and recall. *arXiv preprint arXiv:1806.00035* (2018).
- Tim Salimans, Ian Goodfellow, Wojciech Zaremba, Vicki Cheung, Alec Radford, and Xi Chen. 2016. Improved techniques for training gans. *arXiv preprint arXiv:1606.03498* (2016).
- Omry Sendik, Dani Lischinski, and Daniel Cohen-Or. 2020. Unsupervised K-Modal Styled Content Generation. *ACM Trans. Graph.* 39, 4, Article 100 (July 2020), 10 pages. <https://doi.org/10.1145/3386569.3392454>
- Christian Szegedy, Vincent Vanhoucke, Sergey Ioffe, Jon Shlens, and Zbigniew Wojna. 2016. Rethinking the inception architecture for computer vision. In *Proceedings of the IEEE conference on computer vision and pattern recognition*. 2818–2826.

Ugo Tanielian, Thibaut Issenhuth, Elvis Dohmatob, and Jérémie Mary. 2020. Learning disconnected manifolds: a no GAN's land. In *Proc. ICML*. PMLR, 9418–9427.

Fisher Yu, Ari Seff, Yinda Zhang, Shuran Song, Thomas Funkhouser, and Jianxiong Xiao. 2015. Lsun: Construction of a large-scale image dataset using deep learning with humans in the loop. *arXiv preprint arXiv:1506.03365* (2015).